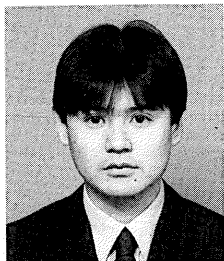


## INFLUENCE OF DESALINATION ON MECHANICAL BEHAVIOR OF PRESTRESSED CONCRETE MEMBERS

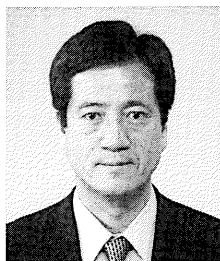
(Translation from Proceedings of JSCE, No.613/V-42, February 1999)



Takao UEDA



Masanobu ASHIDA



Shigeru MIZOGUCHI



Toyo MIYAGAWA

The premature deterioration of concrete structures due to chloride-induced corrosion of reinforcement has recently become a serious problem. Desalination aims to remove chlorides from concrete structures and is expected to enter service as a radical repair method. Desalination has found actual use with RC structures, but application to PC structures has been considered difficult because of the hydrogen embrittlement problem. This paper describes the influence of desalination on the behavior of both prestressing steel bars and PC beams.

**Keywords:** *desalination, electrochemical technique, hydrogen embrittlement, slow strain rate tensile test, hydrogen absorption, flexural test of beam*

---

Takao Ueda is an assistant professor in the Department of Civil Engineering, Tokushima University, Tokushima, Japan. He received his doctorate in engineering from Kyoto University in 1999. His current research interests relate to electrochemical repair methods for deteriorated concrete structures. He is a member of the JSMS, JCI, and JSCE.

---

Masanobu Ashida is a manager in the technical division of the Special Cement Additive Department at Denki Kagaku Kogyo Kabushiki Kaisha Co., Ltd., Japan. His research interests relate to the technology of rehabilitating concrete structures. He is a member of the JSCE.

---

Shigeru Mizoguchi is a manager in the Engineering Sales Section of the Steels and Wire Products Division at Neturen Co., Ltd. His work is related to research and development on prestressing steels, systems, and wire products. He is a member of the JSCE.

---

Toyo Miyagawa is a professor in the Department of Civil Engineering, Kyoto University, Kyoto, Japan. He received his doctorate in engineering from Kyoto University in 1985. He is the author of a number of papers dealing with the durability, maintenance, and repair of reinforced concrete structures. He is a member of the ACI, RILEM, CEB, JSMS, JCI, and JSCE.

---

## 1. INTRODUCTION

It has long been considered that, with adequate design and construction, reinforced concrete structures were extremely durable. However, the early age deterioration of such structures caused by chloride attack has recently become a serious problem. Desalination is an electrochemical repair method that aims to remove chloride ions ( $\text{Cl}^-$ ) from concrete structures. Desalination makes use of currents that are approximately two orders of magnitude higher than those used for cathodic protection, which is the most popular electrochemical method at present. However, desalination has an advantage over other methods in that it is only temporary, unlike cathodic protection.

Examples of the application of desalination to RC structures has been gradually increasing. Recently, the repair effect has been confirmed [1] although some problems are indicated: for example, durability after finishing desalination [2]. On the other hand, there have been few cases of desalination being applied to PC structures because of the problem of hydrogen embrittlement of the prestressing steel.

In this research, the influence of desalination on hydrogen embrittlement of prestressing steel and on the behavior of PC beam members is investigated by applying desalination to pretension-type PC specimens contaminated with chlorides.

## 2. MECHANISM OF HYDROGEN EMBRITTLEMENT

It is assumed that the following cathodic reactions occur around the prestressing steel, which acts as cathode when desalination is applied:



When adequate oxygen exists around the cathode and the cathodic potential is nobler than the hydrogen generation potential, reaction (1) becomes dominant. However, when these conditions are not satisfied, reaction (2) is dominant. The hydrogen generation potential is ignobler than the equilibrium potential calculated by the Nernst Equation but the excess potential, that is the potential difference between this equilibrium potential and the hydrogen generation potential, is affected by current density, temperature, and the surface condition of the steel. As a result, it is not easy to determine the excess potential exactly [3]. From the past research, however, it has been confirmed that the equilibrium potential can be used as the hydrogen generation potential, disregarding the excess potential [4]. Since the pH value of the micro pore solution in sound concrete is generally about 12.5, the equilibrium potential can be calculated as  $-934$  mV vs Ag/AgCl using the Nernst Equation. However, as the pH value around the steel embedded in concrete would increase with the cathodic reaction of desalination, the hydrogen generation potential may be a little ignobler than this level when desalination is applied.

When reaction (2) becomes dominant and hydrogen atoms are generated, these hydrogen atoms diffuse among the crystal lattice of the prestressing steel and accumulate at trapping sites such as dislocations, atomic holes, grain boundaries, and inclusion surfaces. Hydrogen lightly trapped at dislocations, atomic holes, or grain boundaries is known as diffusible hydrogen because it is diffusible at normal temperatures, and this hydrogen is considered to be the direct cause of delayed fractures resulting from hydrogen embrittlement [5]. However, there are a number of theories regarding the mechanism of hydrogen embrittlement, especially the way such trace amounts of hydrogen cause cracking, and the phenomenon remains to be fully clarified.

## 3. TEST PROGRAM

The project described here consists of slow strain rate tensile tests using prestressing steel bars removed from PC prism specimens and flexural tests on PC beams after applying desalination.

The test program is outlined in Table 1. Each experimental factor is examined with two specimens. In this study, all values of current density are referenced to the surface of the prestressing steel bars.

### 3.1 Preparing Specimens and Electric Current Supply

#### a) Mix proportion of concrete

The concrete mix proportion is shown in Table 2. The compressive strength of the concrete reached 40 MPa at the age of 28 days, which was the aim in mix proportion design. Ordinary Portland cement was used, and refined salts (99% NaCl) were used as premixed chlorides. The amount of  $Cl^-$  was  $8.0 \text{ kg/m}^3$ , corresponding to relatively severe chloride attack.

#### b) Prism specimen characteristics

The prism specimens were  $15 \times 15 \times 40$  (cm) with a prestressing steel bar at the center of the square section, and prestressing was by the pretensioning system. In this case, prestress was not introduced to the concrete itself so as to prevent loss of prestress due to creep and drying shrinkage of the concrete, so the prestressing force reaction was supported by the steel form. Three types of prestressing steel were used in the study: two types of PC bars ( $\phi 13$  mm, B-1 type and C-1 type) which had been quenched and tempered by means of high-frequency heating and deformed cold-drawn PC wire ( $\phi 9$  mm). In this paper, C-1 type and B-1 type PC bars are represented by C and B, respectively, and cold-drawn PC wires by CD wire. The mechanical properties and chemical compositions of these prestressing steels are shown in Table 3 and Table 4, respectively. The tension of the prestressing steel was 50% or 60% of its tensile strength. Furthermore, prism specimens made with concrete containing no  $Cl^-$  and non-tensioned PC bars were prepared for reference. An outline of the prism specimen is given in Fig. 1.

#### c) Characteristics of flexural test PC beams

The test beams had a rectangular cross section of width  $10 \text{ cm} \times$  full depth  $20 \text{ cm}$  and a total length of  $160 \text{ cm}$ . A pretensioned PC bar (B or C) was arranged with an effective depth of  $13.3 \text{ cm}$  in the beam section. Moreover, vertical stirrups were provided over the entire shear span at  $10 \text{ cm}$  intervals. Epoxy coated bars D10 SD295A were used as insulated stirrups and erection bars. The loading

**Table 1** Outline of test program

Type of Specimen	Type of Bar	Prestressing Force (%)	Current Density ( $A/m^2$ )	Period of Treatment (weeks)	Period after Treatment	
Prism	B type	0	0.0	8	0	
		50	0.0			
		60	5.0	8	0, 3days, 7days, 1month, 6months, 1year	
			0.0			
			5.0			
			0.0			
	C type	0	0.0	8	0	
		50	0.0			
		5.0				
		60	0.0	4	8	0
			5.0	8		
			0.0	4	8	0, 3days, 7days, 1month, 6months, 1year
5.0	8					
10.0	8		0			
15.0						
CD wire	60	0.0	8	0		
		5.0	8	0, 7days, 1month		
		5.0	8	0		
Beam	B type	50	0.0	8	0	
			5.0			
		60	0.0		8	0, 1month
			5.0			
	C type	50	0.0	8	0	
			5.0			
			0.0			
		60	0.0		8	0, 1month
			5.0			

**Table 2** Mix proportion of concrete

W/C (%)	s/a (%)	NMS (mm)	Unit mass ( $kg/m^3$ )					
			W	C	S	G	AEA	Cl
39	43	25	169	434	731	982	4.67	8

NMS : Nominal maximum size of aggregate

**Table 3** Mechanical properties of PC bars

Type of Bar	Yield Strength (MPa)	Tensile Strength (MPa)	Elongation (%)
B type (SBPR930/1080)	1047	1115	10.0
C type (SBPR1080/1230)	1228	1273	8.0
CD wire (SWPD1L)	1415	1603	6.5

**Table 4** Chemical compositions of PC bars

Type of Bar	Chemical Composition (%)					
	C	Si	Mn	P	S	Cu
B type (SBPR930/1080)	0.35	1.74	0.74	0.016	0.006	0.01
C type (SBPR1080/1230)	0.35	1.74	0.74	0.016	0.006	0.01
CD wire (SWPD1L)	0.82	0.24	0.75	0.012	0.008	0.01

condition of test beams is shown in Fig. 2.

d) Electric current supply procedure

In the case of the prism specimens, concrete was cast around a tensioned PC bar. Then, after curing with a wet mat covering for 28 days, electrodes were placed around the specimen, which was immersed in electrolyte. Then direct current was applied (refer to Fig. 1).

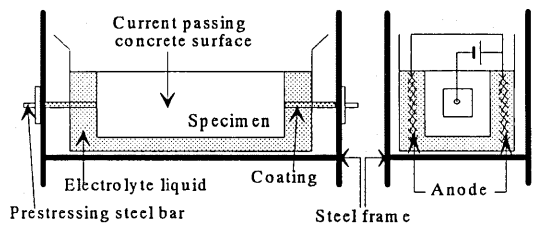


Fig. 1 Prism type specimen

The PC beams were covered with a wet mat after casting for 28 days. After curing, prestress was introduced. Electrodes were then placed around the specimens, which were immersed in electrolyte. Direct current was applied through the PC beams. A saturated solution of  $\text{Ca}(\text{OH})_2$  was used as the electrolyte and titanium mesh plated with platinum formed the anode.

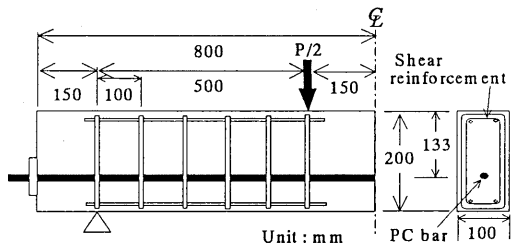


Fig. 2 Beam type specimen

The standard current density was  $5.0 \text{ A/m}^2$  and the standard period of treatment was 8 weeks. Furthermore, certain specimens were treated with a current density of  $10.0 \text{ A/m}^2$  or  $15.0 \text{ A/m}^2$  to investigate the influence of current density. The electric current was passed between two sides of each specimen for the specified period, while the other faces were insulated with an epoxy resin coating. Specimens not subjected to electric current were also kept in the electrolyte solution during the period of treatment.

Specimens used to investigate the influence of elapsed time after finishing treatment were stored with the prestressing force maintained for the specified period (3 days, 1 week, 1 month, 6 months, and 1 year). The storage conditions were a constant  $20^\circ\text{C}$ , 60% R.H.

When the specified treatment and storage were finished, tests were carried out. Prestressing steel removed from the specimens was cooled to a temperature of  $-30^\circ\text{C}$  to prevent evolution of absorbed hydrogen from the prestressing steel.

### 3.2 Slow Strain Rate Tensile Test

Slow strain rate tensile tests were conducted on PC bars or PC wires removed from prism specimens after finishing determined treatment.

a) Test to evaluate delayed fracture sensitivity

The most serious problem caused by the hydrogen embrittlement of high-strength steel is the increase in delayed fracture sensitivity. Tests to evaluate delayed fracture sensitivity can be generally classified into constant load or strain tests and slow strain rate tests (SSRT) [6]. Constant load tests, as represented by the FIP test, estimate the delayed fracture sensitivity by the time taken before cracking or fracture of the steel occurs under a constant load. On the other hand, slow strain tests estimate the delayed fracture sensitivity from certain characteristics of steel obtained through tensile tests with very small strain rates (about  $10^{-6}/\text{sec}$ ).

In this research, the electric current was applied to steel embedded in concrete, not to steel immersed in a solution simulating concrete, and the change in properties of the prestressing steel as it absorbed hydrogen was investigated. A slow strain rate tensile test was selected because it allows for rapid estimation before evolution of the hydrogen.

b) Test procedure

PC bars and wires for test were taken from a freezer immediately before the test and frost was

removed from the steel surface with a cloth. The steel section was not shaved for the test. The fixed strain rate used in tensile testing was  $1.6 \times 10^{-5}/s$ . The load was measured by a load cell with a maximum capacity of 20 tf, and the strain of PC bars and wires was measured with a plastic strain gage. The crosshead displacement of the universal testing machine was measured with a displacement meter which had a maximum capacity of 50 mm (sensitivity: 0.01 mm). Furthermore, the contraction rate of the fractured steel section was defined by the equation below. The sectional area of the fractured steel was measured following JIS Z 2241.

$$\varphi = (A_0 - A) / A_0 \times 100 (\%) \quad (3)$$

where  $A_0$  : original area ( $mm^2$ )  
 $A$  : minimum area of fractured section ( $mm^2$ )

### 3.3 Flexural Testing of PC Beams

Flexural tests were carried out on PC beams after completing the specified treatment as follows.

#### a) Measured points

Load and mid-span deflection were measured by means of a load cell (capacity: 10 tf) and displacement meter (capacity: 25 mm; sensitivity: 0.01 mm), respectively.

Furthermore, to measure crack width at the main reinforcement level ( $d=13.3$  cm) of the flexural span, six 50 mm  $\pi$  gages (capacity: 2 mm; sensitivity: 0.001 mm) were inserted without spaces.

#### b) Loading

Each loading step was 0.25 tf until the yield point, and thereafter, loading was controlled by deflection at mid span; that is, one step was 0.3 mm when the deflection was less than 5 mm, and beyond 5 mm one step was 0.5 mm. When a flexural crack was generated, the beam was unloaded to 0.25 tf once and loaded again until the load reached up to 80% of the maximum load.

All  $\pi$  gages were removed when the gage indication reached about 2 mm. Moreover, the crack spacing at the main reinforcement level was measured after finishing the loading test. The loading conditions for all beams are shown in Fig. 2.

### 3.4 Measurement of Half-cell Potential

Changes with time in half-cell potential of the prestressing steel embedded in the PC beams were measured. As a reference electrode, a saturated silver chloride electrode (Ag/AgCl) was used.

## 4. HALF-CELL POTENTIAL OF PRESTRESSING STEEL

Changes with time in the half-cell potential of prestressing steel embedded in the PC beams were measured for 1 month after 8 weeks of treatment at a current density of  $5.0 A/m^2$ . Results for beams using type C PC bars tensioned to 60% of their tensile strength are shown in Fig. 3. Each line in Fig. 3 correspond to one specimen, and the four divided areas (Non-corrosion, Uncertain, Corrosion, and Protection) shown follow the ASTM criterion for adding cathodic protection area as given by the JCI [7].

From Fig. 3, the half-cell potentials of non-treated specimens were classified in the Uncertain or Corrosion area because PC bars were exposed in the corrosion environment. On the other hand, those of treated specimens just after finishing treatment were

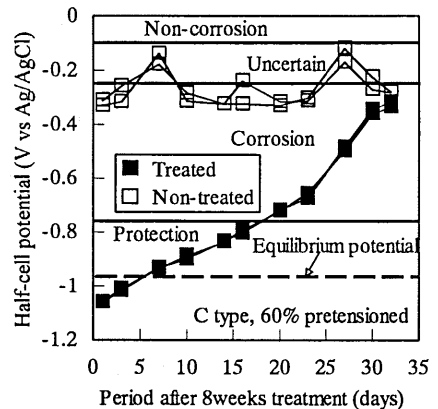


Fig. 3 Change in half-cell potential after 8 weeks of treatment

classified in the Protection area. These potentials classified in the Protection area are ignobler than the hydrogen generation potential because of the strong influence of the electric field. As a result, it is certain that hydrogen was generated during desalination due to the cathodic reaction even if account is taken of the higher pH value around the PC bar, and it is considered that hydrogen embrittlement of PC bar occurred. After stopping the electric current, PC bars were re-passivated with an oxygen supply and potentials gradually became more noble. From Fig. 3, it is seen that half-cell potentials of treated specimens became nobler than the hydrogen generation potential 5 days after desalination ended.

Ishii et al. reported in a study of changes in absorbed hydrogen up to 1 week after stopping the electric current that the peak of diffusible hydrogen absorption into PC wire falls with elapsed time and that the effect of hydrogen embrittlement thus tended to be relieved [5]. At this stage, it is not clear whether there is a relation between the change in half-cell potential after desalination and the relief of hydrogen embrittlement or not. However, it can be said that the risk of delayed fracture due to hydrogen embrittlement decreases rapidly if the half-cell potential remains nobler than the hydrogen generation potential.

## 5. SLOW STRAIN RATE TENSILE TESTS ON PRESTRESSING STEEL

### 5.1 Estimation of Stress-Strain Relation

In this study, the approximate stress-strain curve until the fracture point was obtained by measuring tension load, tendon strain, and crosshead displacement of the universal testing machine during slow strain rate tensile tests.

Generally, the elongation behavior of a steel bar can be divided into two parts. First is the overall elongation that occurs until near the maximum strength point, and second is the local elongation from close to the maximum strength point until the fracture point. Plastic strain gages were used to measure the overall elongation part. However, when local elongation developed in an area not covered by the strain gage, it was impossible to continue measurement of elongation until fracture.

The relations between prestressing steel strain and displacement of the crosshead in the case of the original (as-manufactured) bars and wires are shown in Fig. 4. From this, it can be said that although displacement of the crosshead results in a large relative steel strain in the elastic and early plastic stages because of the reduction in steel bar section, there is a linear relation in the plastic stage of 3% to 5% of steel strain. Beyond this stage, the linear relation is lost due to the dominance of local elongation. In this study, the steel strain after 5% was calculated approximately by means of the linear relation between steel strain and displacement of the crosshead in the 3% to 5% range, and a rough stress-strain curve until the fracture point was obtained. Although each steel bar or wire had its own approximate equation, the range of data used in the approximation was constant (3% to 5% steel strain).

### 5.2 Hydrogen Embrittlement Behavior of Certain Prestressing Steel

Stress-strain curves of specimens treated for 8 weeks and tensioned until 60% of tensile strength are shown in Fig. 5. The influence of treatment on the contraction rate of fractured steel section is shown in Fig. 6. In these figures, data for the original steel are marked as 'Original' for comparison. From Fig. 5, the influence of desalination on elastic behavior and plastic behavior

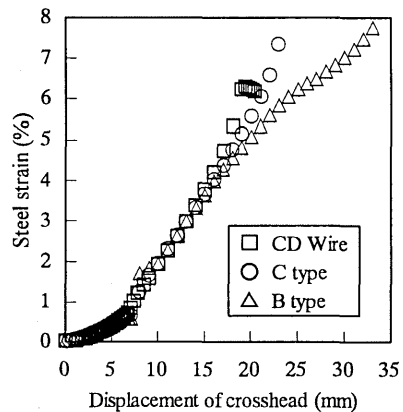


Fig. 4 Relation between steel strain and crosshead displacement (Original bars)

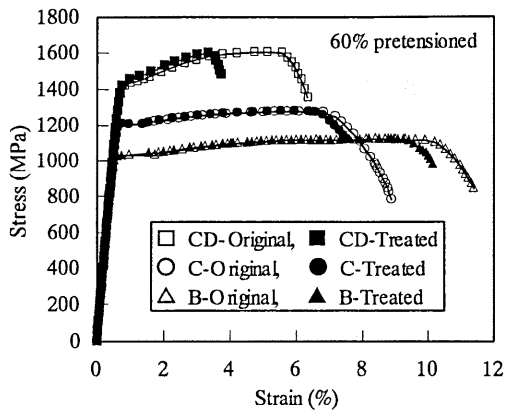


Fig. 5 Influence of treatment on stress-strain relation

before the load begins to decreasing is seen to be very little. From this, it can be said that there is almost no influence of desalination on such characteristics of prestressing steel as elastic coefficient, yield strength, yield strain, and tensile strength. On the other hand, the influence of desalination is clearly visible once the load begins to decrease and up to the fracture point. As a consequence, the ultimate state characteristics, such as strain when the load begins to fall, the length of the load-decreasing zone and contraction ratio of fractured steel section change. As already noted, steel strains in the ultimate state are calculated approximately and it is difficult to estimate the absolute values themselves. However, it is possible to compare them relatively. In both type of B and C cases, the strain of treated specimens when the load begins to fall is a little less than that of the original ones. On the other hand, in the case of CD wire, the strain when the load begins to fall is reduced significantly by treatment. Furthermore, the length of the load-decreasing zone is reduced by treatment for all types of prestressing steel.

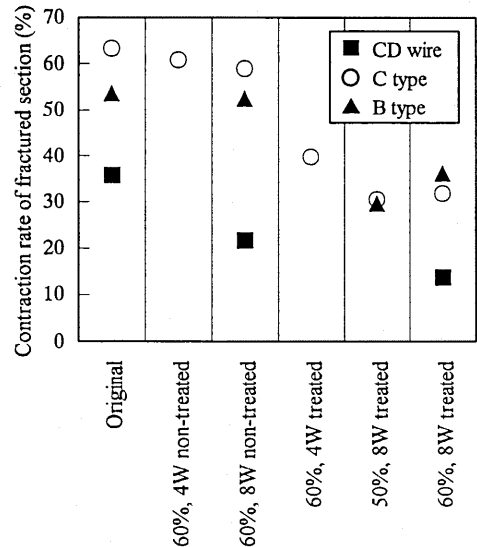


Fig. 6 Influence of treatment on contraction rate of fractured section

From Fig. 6, the contraction rate of the fractured steel section decreases with treatment for all types of prestressing steel and this corresponds to brittle fracturing of the treated specimens as shown in the stress-strain curves. It is deduced that these phenomena are caused by hydrogen embrittlement of the prestressing steel due to the application of desalination, and when the difference in behavior between treated specimens and original ones is considerable, the influence of hydrogen embrittlement and the sensitivity of delayed fracturing is great. Treatment periods for type C specimens were 4 weeks and 8 weeks. The longer treatment results in a greater decrease in contraction rate of fractured steel section, which would correspond to a greater degree of hydrogen embrittlement.

A difference in prestressing force (between 50% and 60% of tensile strength) does not cause a significant change in tension behavior. However, Suzuki et al. reported that when plastic strain was introduced to steel, the absorption of diffusible hydrogen increased because of the generation of trapping sites [8]. The prestressing forces in this study were determined from the permissible tensile stress of prestressing steel under the design load as regulated in the Specifications for Design and Construction of Road Bridges, are premised on the elastic behavior of prestressing steel. However, when desalination is applied to structures that experience very heavy loading, it is possible that the delayed fracture sensitivity becomes high.

The relation between the ratio of treated specimen contraction rate to original one and tensile strength is shown in Fig. 7. The data shown in Fig. 7 were obtained immediately after 8 weeks of treatment and 7 days later. Comparing the delayed fracture sensitivity of heat-treated steel and cold-worked steel, it is generally accepted that cold-worked steel is less sensitive to delayed fracture

than heat-treated steel for the following reasons [9]:  
 · The dense dislocations introduced by cold-working become effective trapping sites for hydrogen.

· The fiber structure of steel introduced by cold working resist the development of cracks in the fracture direction.

On the other hand, if the decrease in contraction ratio means increased delayed fracture sensitivity, Fig. 7 shows that the delayed fracture sensitivity of cold-worked steel is higher than that of heat-treated steel. The reason for this is considered to be that as the heat-treated steel used in this study was quenched and tempered for a short time by high-frequency heating, the binding force of grain boundaries is greater and the delayed fracture sensitivity is lower than that of ordinary tempered martensite steel for the following reasons [10]:

- The crystal grains are fine.
- Film-type cementites are not extracted at the grain boundaries.
- The amount of extracted carbide is little and the extracted carbides are fine.

Moreover, some kinds of steel used in this research have different tensile strengths and as shown in Fig. 7, it can be said as a universal interpretation independent of the steel manufacturing process that the higher strength steel exhibits the higher delayed fracture sensitivity.

Takai et al. conducted FIP tests on PC bars and wires like the prestressing steel used in this study, and the relation between applied stress ratio (applied stress/tensile strength) and time to fracture was as shown in Fig. 8 [9]. This indicates that PC wires has better delayed fracture resistance than PC bars as is generally accepted because the limit of applied stress ratio to fracture is larger for PC wire than for PC bars. However, the time to fracture of PC bars is generally longer than that of PC wire, as seen in Fig. 8. Since the slow strain rate tensile tests used in this study result in steel fracture, there are some important differences from constant load tests like FIP tests and it is possible that time to fracture shown in Fig. 8 is emphasized in slow strain rate tensile tests. Considering this, it is important to evaluate the delayed fracture characteristics of steel from various points of view in the future.

### 5.3 Influence of Pre-mixed $Cl^-$

The main subject of this study is hydrogen absorption caused by electric current treatment, but it has been reported that corrosion reactions can generate hydrogen and that this hydrogen may be a cause of delayed fracture in high-strength steel [11].

In the case of this study, the steel bars removed from treated specimens looked sound and did not appear to be corroded, but bars removed from non-treated specimens were covered with corrosion products. Figure 6 shows that compared with original specimens, non-treated specimens show little decrease of contraction rate of the fractured steel section. Stress-strain curves and contraction rate of the fractured steel section in the case of non-prestressed and non-treated specimens are shown in Fig. 9 and Fig. 10, respectively. In one case, concrete with added chloride

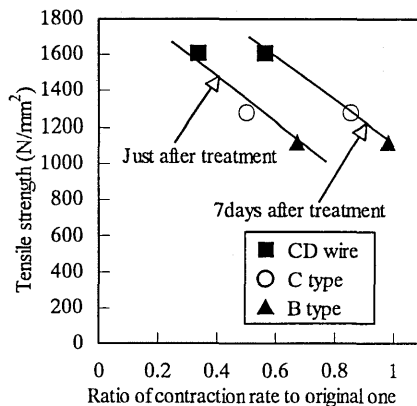


Fig. 7 Relation between contraction rate and tensile strength

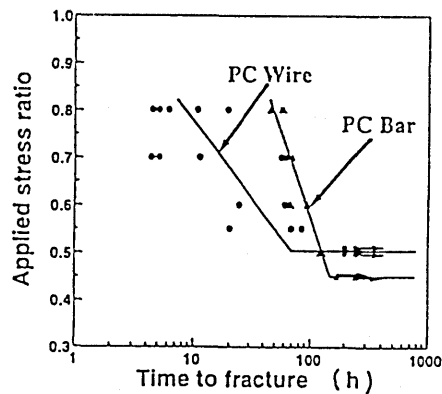


Fig. 8 Relationship between applied stress ratio and time to fracture of PC wire and PC bar in FIP test<sup>9)</sup>

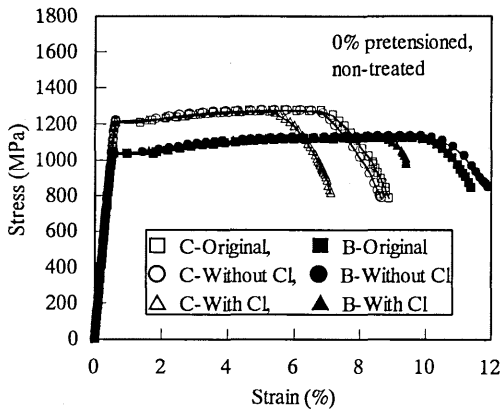


Fig. 9 Influence of  $\text{Cl}^-$  on stress-strain relation

was used and in the other, no chlorides were added. From these figures, it is clear that specimens without  $\text{Cl}^-$  show the same behavior as the original specimens, though in the case of specimens with  $\text{Cl}^-$  the early onset of load reduction and a decrease in the contraction rate are indicated.

From the above, it appears possible that prestressing steel in a corrosive environment absorbs hydrogen generated by the cathode reaction and this hydrogen causes delayed fracture due to hydrogen embrittlement, even if prestressing steel is not influenced by an electric current. There may be some influence of stress corrosion caused by the anodic corrosion reaction, but at present it is difficult to divide these influences clearly.

### 5.3 Influence of High Current Density

For specimens using type C steel tensioned to 60% of tensile strength, the relation between the magnitude of current density and the contraction ratio of fractured steel section is shown in Fig. 11. As the treatment period was 8 weeks in all cases, the higher current density corresponds to the passage of a larger electric charge, so the amount of hydrogen generated by the cathodic reaction should increase in proportion to the current density. However, from Fig. 11, the decrease in contraction rate in the case of specimens treated at a current density of 10.0 and 15.0  $\text{A/m}^2$  is less than that of the specimen treated at a current density of 5.0  $\text{A/m}^2$ . This indicates that at such high current densities, the amount of hydrogen absorbed by the prestressing steel is reduced and the degree of hydrogen embrittlement is relieved.

Batei et al. reported the generation of concrete cracks when an electric current was applied to pretension-type PC specimens in excess of protection requirements [12]. As the cause of this, the expansion pressure of hydrogen gas generated around the steel was suggested [12].

Although no cracks were observed in the concrete surface during this study even when a current density of 10.0 or 15.0  $\text{A/m}^2$  was applied, very fine cracks may be generated around the prestressing steel because of the high current density. Under these circumstances, the amount of hydrogen absorbed by the prestressing steel and the degree of hydrogen embrittlement are likely decreased because the hydrogen pressure is decreased through the generation of such fine cracks.

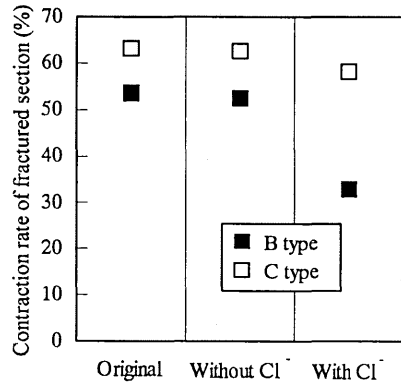


Fig. 10 Influence of  $\text{Cl}^-$  on contraction rate of fractured section (0% pretensioned, non-treated)

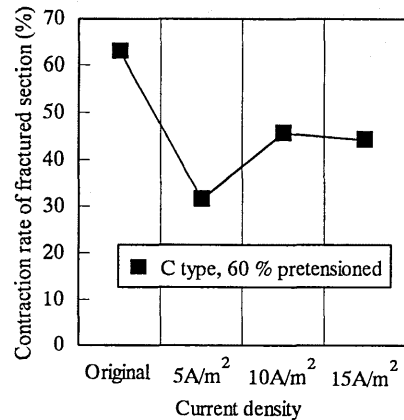


Fig. 11 Influence of current density on contraction rate

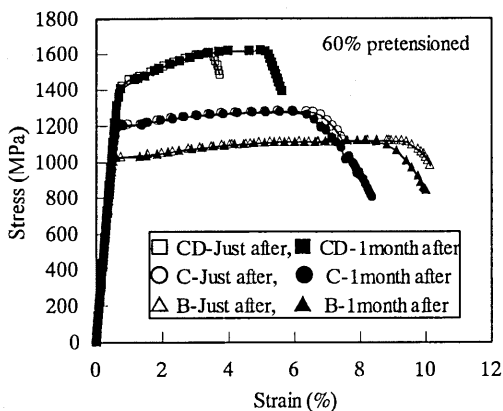


Fig. 12 Influence of time after desalination on stress-strain relation

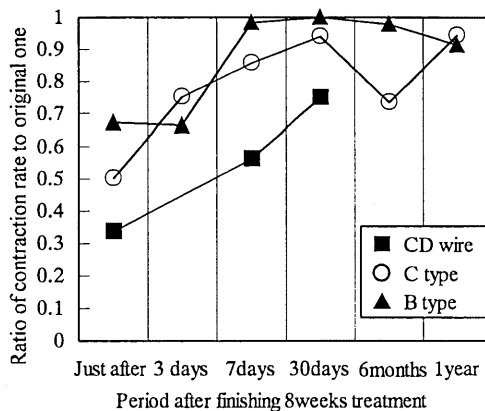


Fig. 13 Influence of time after desalination on contraction rate

#### 5.4 Relief of Hydrogen Embrittlement after Treatment

Suzuki et al. reported a decrease in the amount of diffusible hydrogen absorbed into steel if the steel is kept at room temperature after charging with hydrogen [8]. Since desalination is only a temporary treatment and not a permanent arrangement like cathodic protection, relief of hydrogen embrittlement is expected.

Changes in the stress-strain relation and contraction rate with elapsed time after completion of desalination are shown in Fig. 12 and Fig. 13, respectively. The treatment period was 8 weeks and the prestressing force was 60% of the tensile strength. From Fig. 12, the length of the load decreasing zone, which was reduced under desalination returns to a higher value after 1 month. Moreover, in the case of cold-worked steel, the initial strain at load decrease also rises and as a result the brittle fracture behavior is improved. From Fig. 13, the decrease in contraction rate due to hydrogen embrittlement is relieved with the elapse of time after treatment, regardless of the kind of steel. Thus the contraction rates of heat-treated steels recover to the same level as those of original specimens.

However, the contraction rate of a type C specimen kept for 6 months is smaller than expected. With this specimen, corrosion pits that would have formed during curing were observed, and the fracture originated from this corrosion pitting. It is considered that this brittle fracture was caused by a stress concentration at the pitting and not by hydrogen embrittlement due to desalination.

When desalination is applied to actual structures, there may be corroded prestressing steel present in the structure. In such cases, it is possible that the delayed fracture sensitivity would increase above that of non-corroded prestressing steel, so adequate investigation of this point will be needed in the future.

## 6. FLEXURAL TESTING OF PC BEAMS

Flexural loading tests were carried out immediately after desalination and were completed within 2 days of the end of treatment. After completing desalination, it was not possible to freeze PC beams, so there would have been some evolution of absorbed hydrogen into the prestressing steel. Furthermore, some of the PC beams were tested after 1 month in the room condition.

In the ultimate state, all specimens indicated flexural failure resulting from crushing of the upper concrete. Although it is possible that the prestressing steel might fracture due to hydrogen embrittlement, no such phenomenon was observed in this experiment.

**Table 5** Results of flexural test of PC beams

Type of bar	Prestressing force(%)	Current density (A/m <sup>2</sup> )	Keeping period	Flexural cracking load (kN)	Maximum load (kN)	Average crack spacing (mm)	Number of cracks
C type	60	5	0	51.5	81.1	124	2
				56.2	82.3	150	3
		0	0	52.7	80.1	128	2
	51.7			75.5	125	2	
	46.6			74.5	125	3	
	50	5	0	45.3	77.8	190	2
44.1				72.9	165	2	
0		0	44.9	76.5	202	2	
	60		5	0	46.6	75.4	173
45.0		76.3			188	2	
0		0	46.6	74.1	184	2	
	40.8		75.0	191	2		
	47.0		78.8	188	2		
C type	60	5	1month	50.8	80.9	165	2
				52.7	78.9	229	2
		0	1month	54.6	72.5	202	2
60	5			1month	51.5	77.4	151
		44.8	72.4		177	2	
	0	1month	45.7	68.2	****	1	
45.3			66.1	180	2		

The results for all specimens subjected to the flexural loading test are shown in Table 5.

**6.1 Load-deflection Relation**

Load-deflection relations at the mid span of 60% pretensioned specimens are shown in Fig. 14.

From Table 5 and Fig. 14, it is clear that treatment has a rather the positive influence, slightly increasing flexural rigidity and maximum load as oppose to a negative influence of treatment such as reducing maximum load or increasing deflection. Moreover, the load at which flexural cracking of treated specimens occurs is generally larger than that of non-treated ones. Ishii et al. conducted a static loading test on PC beams with cathodic protection at a maximum current density of 40 mA/m<sup>2</sup> to the steel surface for 3 years [13]. From this, it was observed that the deflection of the treated specimens was less than that of non-treated ones and there was no notable influence of treatment on the load at which flexural cracking occurred and the maximum load. These results obtained by Ishii et al. generally accord with the results obtained in this study.

Ishii et al. concluded that there was no bond degradation as a result of treatment because concrete cracks were not observed along the prestressing steel [13]. However, considering the results of the slow strain rate tensile tests on the prestressing steel itself, which indicated no change

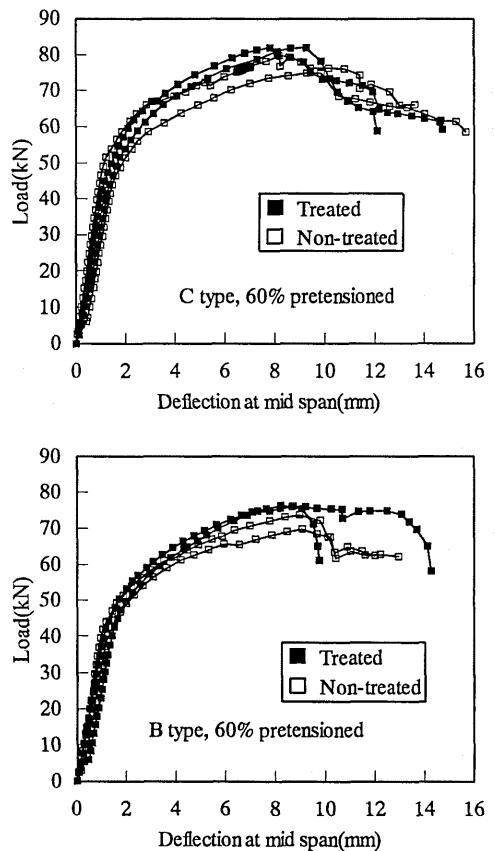


**Fig. 14** Load-deflection relation at mid span

in elastic rigidity or strength due to treatment, it is deduced that desalination does not significantly alter the properties of the prestressing steel itself, and the change in bond interface between concrete and steel influences the mechanical behavior of treated PC beams. Furthermore, from observations of prestressing steel removed from PC beams after flexural loading tests, it was found that corrosion of prestressing steel was slight and it was difficult to imagine a decrease in flexural strength of non-treated PC beams due to corrosion of the prestressing steel.

### 6.2 Cracking Behavior

From the data on average crack spacing and the number of cracks, as given in Table 5, the influence of desalination on the crack distribution is not clear. However, it is not considered that treatment has a negative influence on crack distribution and a small improvement due to treatment is noted.

The road-average crack width relations of the specimens mentioned in Fig. 14 are shown in Fig. 15. The average crack width is the average value for the measured data obtained using the attached  $\pi$  gages across the cracks at the flexural span of the PC beam. These results show that the crack width of treated specimens is generally smaller than that of non-treated specimens under equivalent loading conditions. Thus, since the crack development rate of treated specimens is slower than that of non-treated ones, the deflection of treated specimens is a little less than that of non-treated specimens.

The authors have applied desalination to RC specimens and reported a decrease in bond strength due to the softening of cement paste around the reinforcing steel [14]. Generally, when bond strength decreases, crack width increases because the crack distribution deteriorates. However, as the concrete used in this experiment was relatively high strength compared with RC specimens, the decrease in bond strength may not have been significant. As a result, the crack distribution got no worse and it was possible that the crack development slowed because of the softening of the cement paste around the prestressing steel.

### 6.3 Possibility of Applying Desalination to PC Structures

The results of flexural loading tests on PC beams indicated that there was no negative influence of desalination on the mechanical behavior of PC beams. However, the main problem of hydrogen embrittlement of prestressing steel is the delayed fracture phenomenon, and this experiment does not cover this point adequately enough. Moreover, it is possible that the prestressing steel may be severely corroded when desalination is applied to actual structures. Thus, more investigations including a study of the correlation between hydrogen embrittlement cracking and stress corrosion cracking is needed in the future.

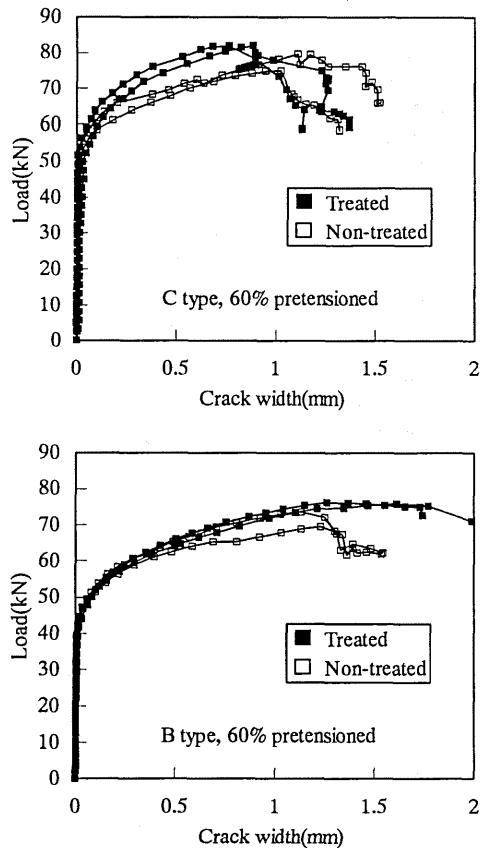


Fig. 15 Load-average crack width relation

## **7. CONCLUSIONS**

The results obtained in this project can be summarized as follows.

- (1) Half-cell potentials of prestressing steel embedded in PC beams treated with desalination for 8 weeks at a current density of  $5.0 \text{ A/m}^2$  were ignobler than the hydrogen generation potential just after finishing treatment. This finding confirmed that hydrogen generation occurred as a result of the cathodic reaction during treatment. However, the half-cell potentials of prestressing steel became nobler than the hydrogen generation potential when the specimens were kept in room condition for 5 days after desalination.
- (2) Slow strain rate tensile tests on prestressing steel removed from treated PC prism specimens indicated no change in elastic behavior nor strength-related properties but the fracture behavior was altered by the absorbed hydrogen. For example, the load decreasing zone in the stress-strain curves was shortened and the contraction rate of the fractured steel section decreased as compared with non-treated specimens.
- (3) As a result of an investigation of the influence of prestressing force of prestressing steel, prestressing forces between 50% and 60% of the tensile strength of each steel type were found to be insignificant.
- (4) As a result of comparing the hydrogen embrittlement behavior of heat-treated PC bars with that of the cold-worked PC wires, the cold-worked steel was found to have severer hydrogen embrittlement behavior in this study. Such a tendency can be interpreted universally in the consideration the tensile strength of steel.
- (5) Prestressing steel embedded in specimens pre-mixed with  $\text{Cl}^-$  showed enhanced brittle fracture behavior in the slow strain rate tensile tests. From this, it was confirmed that prestressing steel under a corrosive environment present the risk of delayed fracture even if there is no influence of hydrogen embrittlement due to electric current.
- (6) As a result of an investigation of the influence of current density applied during desalination, worse hydrogen embrittlement behavior was observed in specimens treated at a current density of  $5.0 \text{ A/m}^2$  than at a density of  $10.0$  or  $15.0 \text{ A/m}^2$ .
- (7) The hydrogen embrittlement of prestressing steels was relieved with the elapse of time when specimens were kept in room condition. From this, it was deduced that the risk of delayed fracture due to hydrogen embrittlement caused by desalination was rapidly reduced, but the risk of delayed fracture originating from corrosion pitting generated before treatment remained.
- (8) As a result of flexural loading tests on treated PC beams, brittle failures such as the fracture of prestressing steel due to hydrogen embrittlement were not observed, and both loading and deflection performance was not reduced by the treatment, compared with the non-treated specimens.
- (9) The average crack width of treated PC beams was a little smaller than that of non-treated specimens for the same loading conditions. As a result, the deflection of treated specimens was a little smaller than that of non-treated specimens.

### **Acknowledgements**

The authors wish to express their sincere gratitude to Mr. N. Tanaka of Neturen Co. Ltd. for his cooperation and helpful advice and to Ms. M. Nishio, Mr. H. Yamaguchi, and Mr. T. Yamashita for their assistance with experiments conducted at the University of Tokushima.

Part of this research was supported by Grant-in-Aid for the Encouragement of Young Scientists from the Ministry of Education (Grant No. 09750544).

## References

- [1] Ueda, T., Ogawa, T., Miyagawa, T., and Ashida, M., "Corrosion Behavior of Reinforcing Steel after Applying Desalination," Proc. of the Japan Concrete Institute, Vol. 18, No. 1, pp.1101-1106, 1996 (in Japanese)
- [2] Bennett, J. E. and Schue, T. J., "Electrochemical Chloride Removal from Concrete: A SHRP Contract Statues Report," Corrosion'90, Paper Number 316, 1990
- [3] Japan Concrete Institute, "Report of Research Committee on Cathodic Protection for Concrete Structures," 1994 (in Japanese)
- [4] Ishii, K., Seki, H., and Fukute, T., "Hydrogen Embrittlement of Prestressing Steel," Journal of Materials, Concrete Structures and Pavement, No. 532/V-30, pp. 131-140, 1996 (in Japanese)
- [5] Suzuki, N., Ishii, N., Miyagawa, T., and Harada, H., "Estimation of Delayed Fracture Property of Steels," Iron and Steel, Vol. 79, No. 2, pp. 227-232, 1993 (in Japanese)
- [6] Suehiro, K., Yamashita, E., Mizoguchi, S., Tanimura, M., and Shimada, T., "Examination of Delayed Fracture Tests on Prestressing Steels," Journal of the Society of Materials Science, Vol. 32, No. 353, pp.94-100, 1983 (in Japanese)
- [7] Japan Concrete Institute, "Guideline for Protection of Marine Concrete Structures (draft)," 1990 (in Japanese)
- [8] Suzuki, N., Ishii, N., and Tsuchida, Y., "Diffusible Hydrogen Behavior in Pre-strained High Strength Steel," Iron and Steel, Vol. 80, No. 11, pp. 855-859, 1994 (in Japanese)
- [9] Takai, K., Seki, J., and Homma, Y., "Hydrogen Occlusion Behavior during Delayed Fracture in Cold Drawn Steel Wire and Heat Treated Steel Bars for Prestressed Concrete," Iron and Steel, Vol. 81, No. 10, pp. 1025-1030, 1995 (in Japanese)
- [10] The Iron and Steel Institute of Japan, "Advance of Research on Delayed Fracture," 1997 (in Japanese)
- [11] Ikeno, K., Nishimura, R., and Yamakawa, K., "Hydrogen Absorption of Carbon Steel under Corrosion Atmosphere," Proc. of the 42th Conference on Corrosion and Protection, pp.565-568, 1995 (in Japanese)
- [12] Batei, S. and Takewaka, K., "Application of Cathodic Protection for Prestressed Concrete Structure," Proc. of the 46th Annual Conference of the Japan Society of Civil Engineers 5, pp.360-361, 1991 (in Japanese)
- [13] Ishii, K., Seki, H., Fukute, T., and Ikawa, K., "Experimental Study on Pretension PC Beam Given Cathodic Protection," Proc. of the 22th JUCC Congress on Cement and Concrete, pp.91-96, 1995 (in Japanese)
- [14] Ueda, T., Hattori, A., Ashida, M., and Miyagawa, T., "Influence of Desalination on Bond Behavior between Concrete and Reinforcing Steel," Journal of Materials, Concrete Structures and Pavement, No. 550/V-33, pp. 53-62, 1996 (in Japanese)